



Effect of Ultrasonic Power on Water Removal Kinetics and Moisture Migration of Kiwifruit Slices During Contact Ultrasound Intensified Heat Pump Drying

Yunhong Liu¹ · Ya Zeng¹ · Xiaoyue Hu¹ · Xue Sun¹

Published online: 3 January 2020
© Springer Science+Business Media, LLC, part of Springer Nature 2020

Abstract

The experiments of contact ultrasound intensified heat pump drying (CUHPD) of kiwifruit slices were conducted to investigate the effect of ultrasonic power on dehydration process and water migration of kiwifruit during CUHPD. The results clarified that contact ultrasound (CU) application could reduce the drying time of HPD significantly, and the rise of ultrasonic power had stronger reinforcing effect on dehydration rate. Weibull distribution function could simulate the dehydration process of CUHPD of kiwifruit with high precision, and the β values verified that ultrasonic power improvement could transform the moisture diffusion mechanism of CUHPD from total internal moisture diffusion control to partial internal moisture diffusion control. The D_{cal} values were $2.304 \times 10^{-9} \sim 4.026 \times 10^{-9} \text{ m}^2/\text{s}$ and increased as the rise of ultrasonic power. The scanning electron microscopy results illustrated that increasing ultrasonic power could produce more porous and spacious microstructure which was beneficial for water migration. The low-field nuclear magnetic resonance results elucidated that free water, immobilized water, and bound water in kiwifruit migrated and changed during CUHPD. Free water with the highest mobility was the most abundant water in kiwifruit, and was the first kind of water to be completely removed. With drying progressed, the contents of immobilized water and bound water gradually increased and then decreased, but they were not completely removed. The increasing in ultrasonic power was beneficial to promoting internal water migration and shortening the required dehydration time, especially for free water. Proton density images visualized that increasing ultrasonic power could significantly promote the water diffusion from internal kiwifruit outward the surface, and thereby accelerate the rate of water removal. Therefore, CU application is a suitable method to accelerate the water diffusion and moisture migration of HPD process.

Keywords Ultrasonic power · Heat pump drying · Kiwifruit · Water status · Moisture migration · Low-field nuclear magnetic resonance

Introduction

Kiwifruit (*Actinidia chinensis* Planch.) is a favorite and familiar fruit in the world (Izli et al. 2017). Kiwifruit contains a large amount of sugar, protein, amino acids, and a variety of minerals and vitamins necessary for human body, and has high nutritional and healthy functions (Nowacka et al. 2018). As a kind of berry fruit, kiwifruit is prone to decay or deteriorate due to the action of microorganisms and enzymes

during storage (Akar and Barutçu Mazı 2019). Therefore, making kiwifruit into dried products is a good way to prolong its storage period and improve its market value. Hot air-drying is a frequently used means for kiwifruit drying (Darıcı and Şen 2015), but it has several disadvantages including lengthy time and low efficiency. Freezing drying is a favorable method to obtain dried kiwifruit with high quality; nevertheless, high energy consumption and too long drying period limit the popularization of freezing drying (Çalışkan et al. 2015). Thus, a suitable drying method with low energy consumption and high dehydration rate should be applied for kiwifruit drying.

Heat pump drying (HPD) is a modern drying method that converts low-grade thermal energy into high-grade heating energy by heat pump system, and provides thermal energy for dried materials, and has the advantages of high efficiency, energy saving, and good product quality (Liu et al. 2014;

✉ Yunhong Liu
lyunhong@hotmail.com

¹ School of Food and Bio-Engineering, Henan University of Science and Technology, Luoyang 471000, China

Mohammadi et al. 2019). HPD has been successfully used for dehydrating many agricultural products and foodstuffs including carrot (Sun et al. 2017b), soybean seed (Zhao et al. 2017), ginger (Chapchaimoh et al. 2016), and cocoa bean (Hii et al. 2012). These researches verified that HPD could realize low energy consumption and high product quality. However, kiwifruit has compact microstructure and complex tissue and contains many sugars and colloid substances with strong absorption capacity of water (Akar and Barutçu Mazi 2019), and hence, the whole drying processes of kiwifruit are usually reflected as internal diffusion-controlled property in most cases. HPD has the characteristic of external heating, which has no obvious effect on improving internal mass transfer process. Therefore, it would be appropriate to employ an effective method in HPD to reduce internal mass transfer resistance and promote moisture diffusion and migration inside materials.

Contact ultrasound (CU) technology has been paid more and more attention in strengthening drying process (García-Pérez et al. 2009; Liu et al. 2019). CU technology is the application of an ultrasound device that can transmit mechanical waves with wavelength of higher than 20 kHz and achieve the matching of ultrasonic transducer, radiation plate, and materials (Liu et al. 2017). During CU treatment, the generated ultrasonic energy can transmit into dried samples directly from an ultrasound radiator without relying on any media, and then can improve ultrasonic utilization rate and promote dehydration rate. Liu et al. (2015 and 2019) conducted hot air-drying experiments of pear slices with air-mediated ultrasound (Liu et al. 2015) and CU (Liu et al. 2019) and the compared results indicated that CU could achieve higher dehydration rate and shorter drying time at lower ultrasonic power. Tao et al. (2019) revealed that CU application in hot air-drying of cabbage could significantly shorten drying time by intensifying internal water diffusion. Liu et al. (2017) confirmed that effective moisture diffusivity and product quality could be improved when CU strengthening technology was applied in hot air-drying of sweet potato. Musielak et al. (2016) also announced that CU application in drying was conducive to shortening dehydration period and reducing total energy consumption. Hence, the CU application can theoretically promote mass transfer of kiwifruit during HPD. However, the study on contact ultrasound intensified heat pump drying (CUHPD) of kiwifruit is scarce.

Nowadays, several studies have reported the ultrasound application in drying of different kinds of food materials including beetroot (Vallespir et al. 2018), mushroom (Vallespir et al. 2019), apple (Fernandes et al. 2015), orange peel (García-Pérez et al. 2012), and so on. These published studies mainly focus on the drying rate and some quality parameters. As water is a very important component in foodstuff which can affect the processing characteristics, low-field nuclear magnetic resonance (LF-NMR) technology and magnetic

resonance imaging (MRI) have been increasingly adopted to determine the status of water within food materials (Lv et al. 2017; Sun et al. 2019). But there are only few studies elucidating the water status information in the application of ultrasound prior to drying process (Jiang et al. 2018; Rodríguez et al. 2015). Rodríguez et al. (2015) studied the effects of ultrasound assistance during the predrying treatment of apple using LF-NMR. Their results showed that ultrasound treatment could result in greater mobility of internal water and easier water removal during convective drying. It is of importance for revealing water removal and status change during drying process. However, there is a lack of published information about the effects of CU application on water status and moisture transfer during the whole HPD process. Moreover, since ultrasonic power is one of the most important parameters in ultrasound strengthening application in drying process, the influence of ultrasonic power on moisture migration during CUHPD of kiwifruit is unclear and needs to be explored.

Therefore, the target of this research was to explore the effect of CU on water removal process, microstructure, water change, and moisture migration during HPD of kiwifruit. Drying characteristics of CUHPD of kiwifruit at different ultrasonic powers were discussed and Weibull distribution function was applied for simulating the dehydration process of CUHPD. Microstructure photographs of CU-treated surface and internal microstructure of kiwifruit dried at different ultrasonic powers were analyzed by scanning electron microscopy (SEM). Water status changes and moisture migration in CUHPD were explored by LF-NMR technology and MRI method.

Materials and Methods

Material

Fresh kiwifruits were bought at a local market in Luoyang, China. The fresh kiwifruit's moisture content was measured as 6.54 ± 0.26 g/g (d.b.) by vacuum-drying method (AOAC 1990).

CUHPD Equipment

The CUHPD equipment was achieved by installing a self-fabricated contact ultrasound device in an HPD equipment (GHRH-20, Guangdong Agricultural Machine Research center, China), and the scheme of CUHPD equipment is illustrated in Fig. 1. The detailed structure and working mechanism of the HPD equipment was reported in the previous research (Liu et al. 2014).

The contact ultrasound device was mainly composed of an ultrasonic transducer and ultrasonic generator, and the appearance is presented in Fig. 2. The ultrasonic generator is an

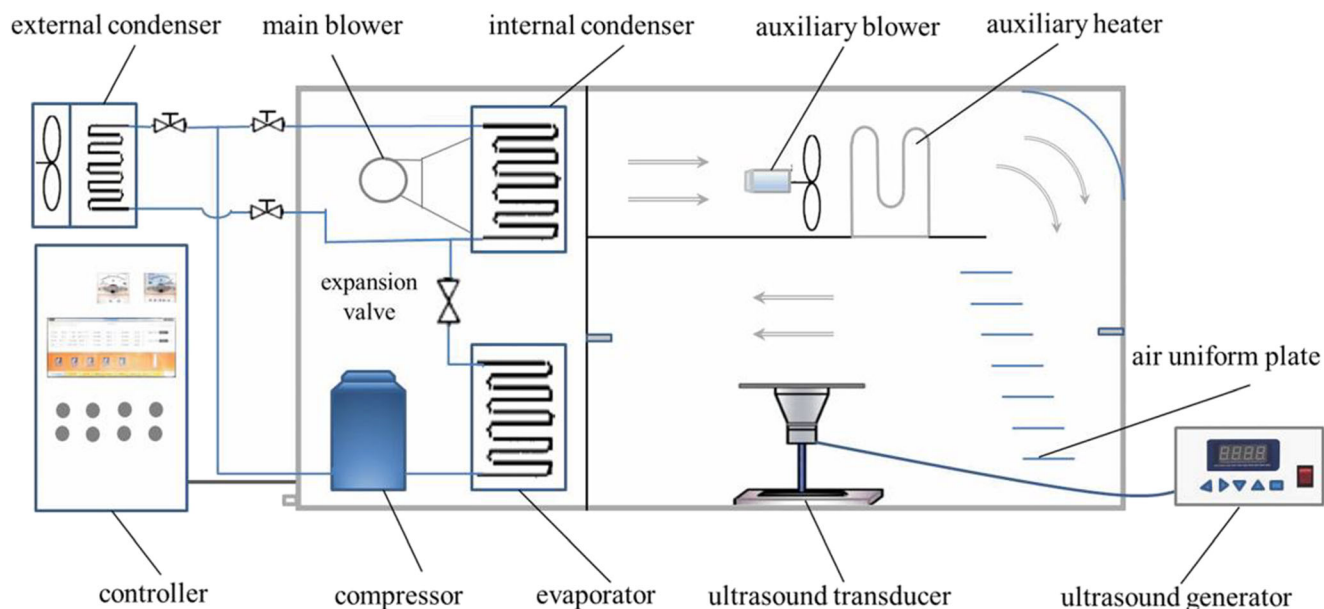


Fig. 1 Schematic of CUHPD equipment

important component of the ultrasonic system, and ultrasonic oscillator is the core component of ultrasonic generator. The function of ultrasonic oscillator is to generate a constant frequency signal and drive the amplifier part. In this study, the structure of He-type oscillator circuit was adopted for the ultrasonic generator to achieve stable ultrasound oscillation frequency and wide bandwidth adjustment range. The trumpet-shape piezoelectric transducer was adopted due to its low dielectric loss and good impedance matching capability, and could convert electrical signals into acoustic signals. The stainless-steel ultrasonic vibration plate was bonded to the upper surface of the ultrasonic transducer by special viscose. If the vibration plate is thin or small, the energy transferred by transducer will be easily converted into heat energy, which could cause the overheating and cavitation corrosion of vibration plate. If the vibration plate is thick or large, the energy transmitted by transducer will be absorbed by vibration plate, and the energy generated will be greatly reduced. After several

tests, the vibration plate with 2 mm in thickness and 150 mm in diameter could well match the ultrasonic transducer. After ultrasonic generator is turned on, the ultrasonic power of ultrasound can be adjusted from 0 to 60 W by the “+” and “-” buttons on the generator panel. The ultrasonic generator transfers the high-frequency electric energy generated by the ultrasonic generator to the transducer. The ultrasonic transducer converts the electric energy into sound energy. The sound energy generated is transmitted to the vibration plate and causes the vibration of plate in high frequency and small amplitude, and then transmits the ultrasonic energy to the interior of material. The frequency of the ultrasonic system could be adjusted in the range of 20–100 kHz. In order to determine the resonance frequency of the ultrasonic system, a certain amount of water was sprayed on the material vibration plate, and the ultrasonic generator was turned on to observe the vibration height and intensity of water on the vibration plate at different ultrasonic frequencies. The strongest turbulence



Fig. 2 Photograph of the ultrasound system

and vibration intensification of water could be observed at 28 ± 0.5 kHz. Then, some pre-experiments were conducted to verify that the greatest reinforcement effect of ultrasound on HPD process of kiwifruit could be achieved at ultrasonic frequency of 28 kHz; therefore, such an ultrasonic frequency value was fixed in the subsequent drying experiments.

Drying Methods

Kiwifruit samples were cut as slices with 6 cm in diameter and 0.4 cm in thickness with a food slicer. About 80 g kiwifruit slices were put on the ultrasonic board uniformly in drying experiments. The ultrasonic powers in this study were set as 0, 18, 36, and 54 W (the corresponding ultrasonic power densities were 0, 0.1, 0.2, and 0.3 W/cm²), respectively. The mass values of kiwifruit samples during CUHPD were measured by a digital balance (BSA323S, Sartorius Co., Germany) at 30-min intervals. In order to well investigate the influence of CU on dehydration process and water migration, the air velocity and air temperature in CUHPD were fixed as 1.5 m/s and 40 °C, respectively. Each experiment was carried out in triplicates.

The sample's moisture content M in CUHPD process can be obtained according to Eq. (1) (Liu et al. 2015; Winiczenko et al. 2018):

$$M = \frac{W - W_d}{W_d} \quad (1)$$

where W is sample mass (g), W_d is dry matter's mass (g).

Weibull Distribution Function

The moisture ratio (MR) could be obtained as follows (Rojas and Augusto 2018; Kek et al. 2013):

$$\text{MR} = \frac{M_t - M_e}{M_0 - M_e} \quad (2)$$

where M_t is moisture content at drying time t , M_0 is initial moisture content, and M_e is equilibrium moisture content and usually could be negligible (g/g, d.b.).

The proposed model for the simulation of the drying curve in CUHPD of kiwifruit was the Weibull distribution function, which has been frequently used for the prediction of drying process (Corzo et al. 2010; Weibull 1951):

$$\text{MR} = \exp \left[- \left(\frac{t}{\alpha} \right)^\beta \right] \quad (3)$$

where α is the scale parameter (min), and β is the shape parameter.

Two criteria were applied to assess the model's accuracy: the coefficient of determination (R^2) and root mean square error (RMSE) between the predicted and experimental values.

The R^2 and RMSE were calculated as follows, respectively (Corzo et al. 2010; Uribe et al. 2011):

$$R^2 = 1 - \frac{\sum_{i=1}^N (MR_{\text{pre},i} - MR_{\text{exp},i})^2}{\sum_{i=1}^N (MR_{\text{exp},i} - MR_{\text{exp},i})^2} \quad (4)$$

$$\text{RMSE} = \left[\frac{1}{N} \sum_{i=1}^N (MR_{\text{pre},i} - MR_{\text{exp},i})^2 \right]^{\frac{1}{2}} \quad (5)$$

where N is the number of experimental data points, and MR_{exp} and MR_{pre} are experimental and predicted values, respectively.

The calculated diffusion coefficient D_{cal} , which is originated from Weibull function and represents moisture diffusivity during drying, could be obtained as follows:

$$D_{\text{cal}} = \frac{L^2}{\alpha} \quad (6)$$

where D_{cal} is the calculated diffusion coefficient (m²/s), L is the thickness of kiwifruit slice (m), and α is the scale parameter of Weibull function (s).

SEM

The dried sample's microstructure was analyzed by a scanning electron microscopy (JSM6010LA, JEOL Co., Japan). One kiwifruit specimen was cut from the ultrasound radiated surface of kiwifruit samples and another specimen was cut from internal section of kiwifruit slice, and the specimens were put on a stainless stub and gold sputtered. The SEM observations for ultrasound-treated surface and internal microstructure of kiwifruit slices were conducted at $\times 300$ magnifications and $\times 200$ magnifications, respectively.

LF-NMR

The measurements of transverse relaxation were investigated using a NMI20-015V-I NMR analyzer (Niumag Electric Co., Shanghai, China), which was conducted at a resonance frequency as 21.0 MHz at 32 °C. The sample's transverse relaxation time (T_2) was obtained by Carr-Purcell-Meiboom-Gill pulse sequence with 8 scans, 18,000 echoes, and 0.5 ms between pulses of 90° and 180°. The T_2 inversion spectrums were performed using inversion software (Niumag Electric Co., Shanghai, China) for each process, and the area under each peak was determined by cumulative integration.

MRI Measurement

The proton density weighted images are also acquired on the LF-NMR analyzer. The multiple spin-echo imaging sequence parameters are as follows: slice gap 0.5 mm, slice width

2.5 mm, average 4, phase size 192, read size 256, echo time (T_E) 20 ms, repetition time (T_R) 500 ms.

Statistical Analysis

Data analysis and ANOVA were carried out with Origin 2018 software.

Results and Discussion

Drying Curves

The CU enhancements were applied in HPD of kiwifruit at 40 °C with ultrasonic powers of 0, 18, 36, and 54 W, respectively, and the corresponding moisture content change curves are depicted in Fig. 3. The drying time of single HPD without ultrasonic enhancement (0 W) was 450 min, while the needed drying times could be reduced as 360, 300, and 240 min at ultrasonic powers of 18, 36, and 54 W, with the decreasing ratios of 20%, 33%, and 46%, respectively. The phenomena above indicated that the CU application in HPD drying of kiwifruit slices could achieve obvious drying reinforcement effect, and higher ultrasonic power could produce stronger reinforcement effect and then shorter dehydration time. In the process of CUHPD drying, kiwifruit slices were directly put on the ultrasonic radiation board. The ultrasound wave can straightly penetrate into the materials (Liu et al. 2019). Numerous microbubbles could be produced by ultrasound treatment inside kiwifruit's tissue liquid, and the generation and explosion of these bubbles could produce strong impact and oscillation (Musielak et al. 2016). Ultrasound energy could also cause high-frequency vibration and turbulence inside kiwifruit samples, and then

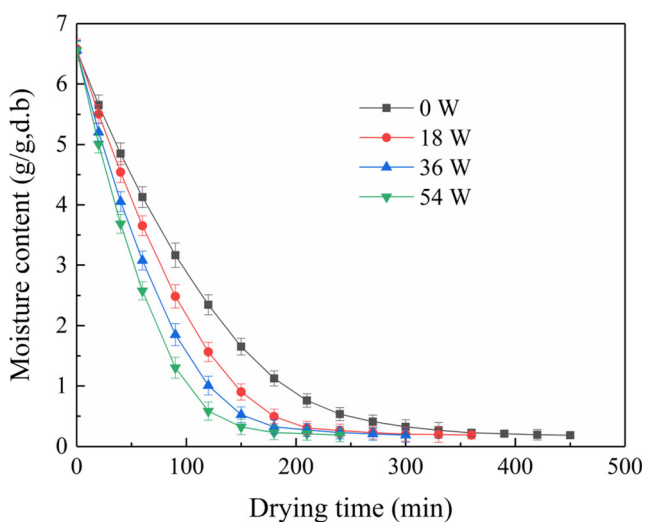


Fig. 3 Moisture content change of kiwifruit during CUHPD at different ultrasonic powers

reduce water adsorption capacity and improve moisture fluidity (Schössler et al. 2012). The above ultrasonic effects could be beneficial for water diffusion as well as dehydration process. With the rise in ultrasonic power, stronger ultrasonic reinforcing effects on water diffusion and mass transfer could be produced to realize shorter drying time. Tao et al. (2019) also found that the improvement of ultrasonic power can accelerate internal moisture diffusion and then promote drying rate during hot air-drying of cabbage.

Weibull Distribution Model

Weibull distribution function was applied to fit the moisture content change curves of CUHPD of kiwifruit, and the results are listed in Table 1. The range of determination coefficients (R^2) was 0.9916–0.9951, and the range of root mean square error (RSME) was 0.0085–0.0162. All the R^2 values were close to 1, and all the values of RMSE were extremely small. Hence, the result elucidated that Weibull distribution model was appropriate for predicting moisture content change of kiwifruit during CUHPD.

The scale parameter α represents the time needed for accomplishing around 63% of the drying process (Marabi et al. 2003). The α value decreased with the rise of ultrasonic power. For example, the α value was 115.714 min at 0 W and it reduced to 62.208 min as ultrasonic power increased to 54 W, with the corresponding reduction ratio of 46%. The result indicated that CU treatment had a remarkable influence on the α values and drying period, and increasing ultrasonic power could improve α value as well as dehydration rate.

The shape parameter β is related to the moisture migration mechanism during drying process (Uribe et al. 2011). When $\beta < 1$, the drying is dominated by internal water diffusion. When $\beta > 1$, the drying is governed by both internal moisture diffusion and external mass transfer (Corzo et al. 2010). The β values increased from 0.972 to 1.112 as ultrasonic power increased from 0 to 54 W. The phenomenon implied that single HPD process belongs to internal moisture diffusion control with great internal mass transfer resistance, and the increase of ultrasonic power in CUHPD could transform the moisture diffusion mechanism from total internal moisture diffusion control to partial internal moisture diffusion control by significantly reducing internal water diffusion resistance.

Table 1 Fitting parameters and fitting precision indexes of Weibull distribution function

Ultrasonic power (W)	α (min)	β	R^2	RMSE	D_{cal} (m^2/s)
0	115.714	0.972	0.9916	0.0162	2.304×10^{-9}
18	91.286	1.069	0.9922	0.0141	2.921×10^{-9}
36	74.762	1.086	0.9951	0.0116	3.567×10^{-9}
54	62.608	1.112	0.9943	0.0085	4.026×10^{-9}

D_{cal} Values

The D_{cal} values of CUHPD of kiwifruit are presented in Table 1. The range of D_{cal} was $2.304 \times 10^{-9} \sim 4.026 \times 10^{-9} \text{ m}^2/\text{s}$. It is also expressed that D_{cal} values rose with the ultrasonic power's improvement. The ultrasound treatment could increase the turbulence of water inside the material, reduce the adhesion on the micro-tubes, improve the degree of water freedom in the material, accelerate water movement, and thereby increase diffusion rate and D_{cal} values. Ortuño et al. (2010) also confirmed that CU application could increase mass transfer coefficient as well as water diffusivity during orange peel's hot air-drying process.

SEM

The SEM images of the ultrasound-treated surface and internal microstructure of kiwifruit slices after CUHPD at different ultrasonic powers are illustrated in Figs. 4 and 5, respectively. It could be observed that both the surface structure and interior structure of kiwifruit are compact with only several microtunnels after HPD without CU application. This kind of compact structure may be due to the continuous contraction accompanied by ongoing water removal, and such a compact structure could hinder outward diffusion of internal moisture (Liu et al. 2019). After CU application, it could be observed

that both the microstructure of ultrasound-treated surface and the interior microstructure of kiwifruit became loose and porous, and higher ultrasonic power could bring about more micropores and larger microtunnels. The phenomenon indicated CU treatment can strengthen water turbulence and internal vibration, and then decrease cell tissue contraction and protect mass transfer pathways (Musielak et al. 2016). Higher ultrasonic power led to more porous and spacious microstructure not only at the treated surface but also inside kiwifruit slices, which was beneficial for the outward migration and diffusion of internal water. The influence of ultrasonic power on water status and water migration during HPD could be further analyzed by LF-NMR.

T_2 Relaxation Spectra

According to the principle of NMR, different chemical environment of protons can lead to various relaxation times as well as different freedom degree of water (Li et al. 2014). Shorter relaxation time represents closer binding between water and material, lower freedom degree of proton, and weaker moisture mobility (Li et al. 2018; Wei et al. 2018). T_2 can indirectly reflect the phase characteristics of water and the change of T_2 can express the fluidity of water molecules. The signal amplitude covered by different T_2 peaks can represent the relative content of hydrogen protons in each interval. Therefore, the

Fig. 4 SEM images of dried kiwifruit slices at different ultrasonic powers: **a** 0 W, **b** 18 W, **c** 36 W, **d** 54 W

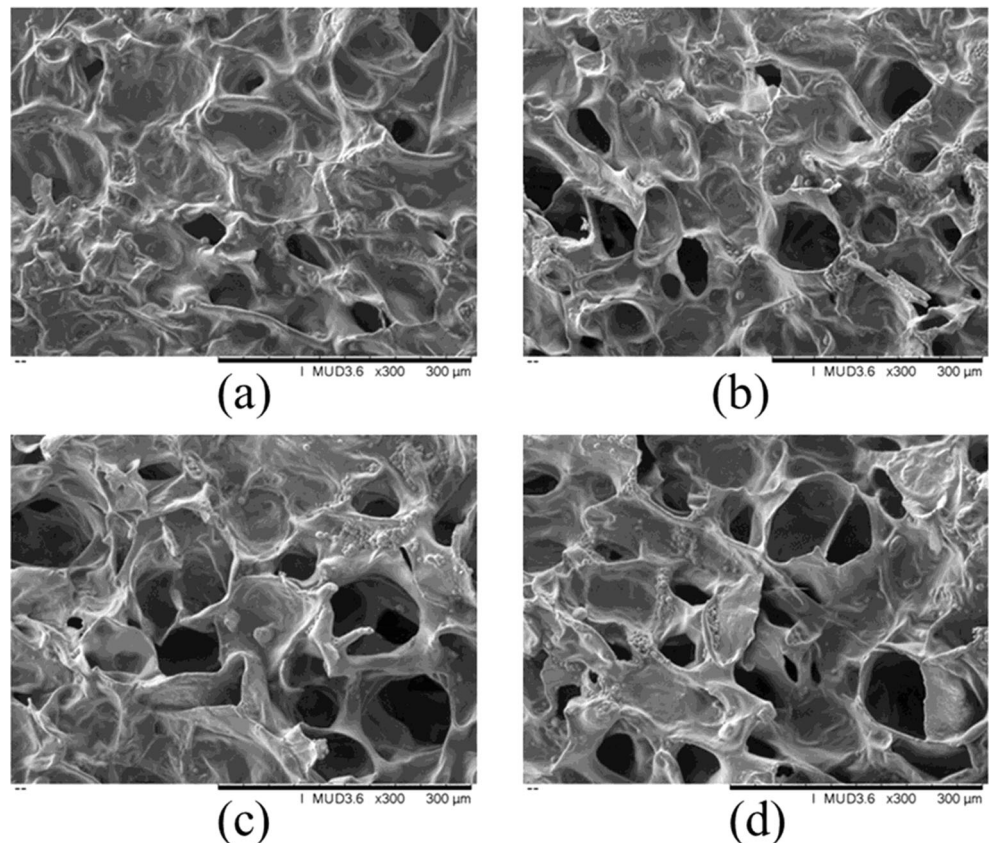
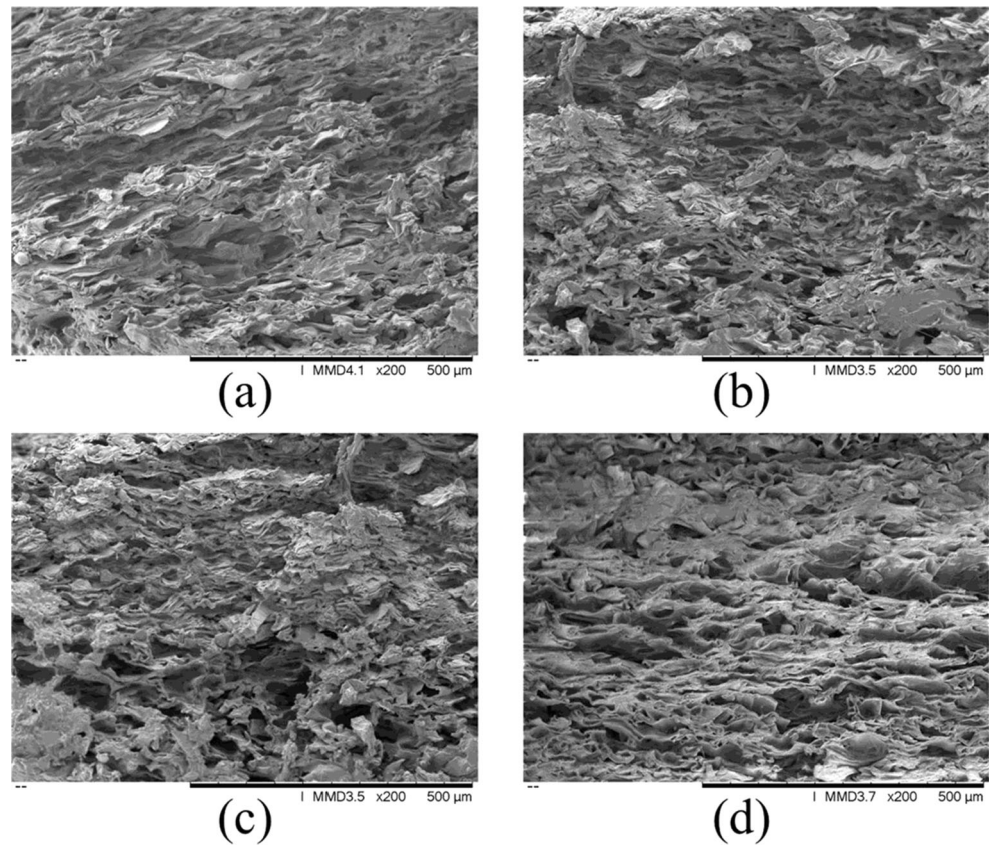


Fig. 5 SEM images of internal microstructure of dried kiwifruit slices at different ultrasonic powers: **a** 0 W, **b** 18 W, **c** 36 W, **d** 54 W

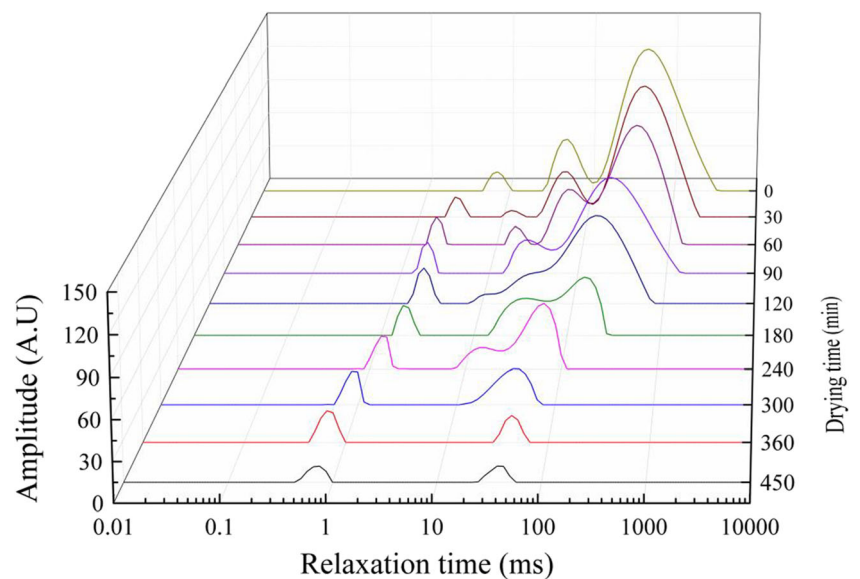


water status change and moisture migration law during drying can be described and analyzed based on T_2 relaxation spectra.

Figure 6 demonstrates the variation of relaxation spectra of kiwifruit slices during HPD process. There are three peaks in the inversion spectrum of kiwifruit, which can represent three different water states in kiwifruit. The relaxation spectra can be divided into three zones: T_{21} (0.01–10 ms), T_{22} (10–

100 ms), and T_{23} (> 100 ms), which represent bound water, immobilized water, and free water, respectively. The distribution characteristics of transverse relaxation time in samples are closely related to the properties of cell tissues. The longer the transverse relaxation time was, the greater the degree of freedom of protons was and the stronger the mobility of water was (Lv et al. 2018). The shortest relaxation time, T_{21} , represents

Fig. 6 T_2 relaxation spectra of kiwifruit slices during HPD process



bound water that binds closely to the macromolecular substances such as proteins and polysaccharides through hydrogen bonds. T_{22} represents immobilized water that exists in the cytoplasm and intercellular space and is bound by certain binding force. The maximum area of T_{23} corresponds to free water located in surface and vacuole and between fibrous tissues with high mobility.

According to the inversion spectrum, fresh kiwifruit had the largest corresponding NMR signal amplitude, indicating that fresh kiwifruit had the highest moisture content. The amplitude of T_{23} was significantly higher than that of T_{22} and T_{21} , which meant that the moisture content of fresh kiwifruit was mostly free water, and the contents of immobilized water and bound water were much less. As the drying process went on, the total peak area of inversion spectrum decreased, and the whole inversion spectrum shifted to the left side to a certain extent. It was demonstrated that the moisture content in kiwifruit decreased, and the moisture content changed from high degree of freedom to low degree of freedom, and the degree of water-solid bonding in the sample increased (Li et al. 2014). In the early stage of drying, because of the good fluidity of free water, free water was most easily removed from kiwifruit during drying, which led to the continuous left movement of T_{23} and the rapid decrease of peak amplitude. With the drying process, the free water decreased continuously until it was completely removed. There was still some immobilized water and bound water in kiwifruit slices, and the peak amplitude and transverse relaxation time of T_{21} and T_{22} began to decrease gradually, and the removal of immobilized water was greater than bound water. Throughout the drying process, the relaxation time of T_{21} changed much less than that of T_{22} and T_{23} , which represented that the binding forces between bound water and macromolecule matter were very stable, and the influence of drying process on bound water was much weaker than that on free water and immobilized water (Wei et al. 2018). At the end of drying, the bound water was the main component accompanied by a small amount of immobilized water inside kiwifruit, while free water could not be observed completely.

Changes of Water Status and Water Proportion

Based on the total signal intensity change of water in different states in T_2 inversion spectrum, the relative contents of different water states in dehydration process can be obtained, and the proportion change of each component water can be calculated. In the CUHPD process of kiwifruit, the peak areas of free water, immobilized water, and bound water under different ultrasonic powers are shown in Fig. 7, and the corresponding peak area proportions are presented in Fig. 8.

It is illustrated from Fig. 7 that the free water of kiwifruit shows a downward trend in CUHPD process at all ultrasonic power levels. When ultrasonic powers were 0, 18, 36, and

54 W, the total removal times for free water were 270, 180, 150, and 120 min, respectively, indicating that the higher the ultrasonic power was, the quicker the migration speed of free water was and the shorter the removal time was. It is shown from Fig. 8 that higher ultrasonic power could lead to faster reduction of peak ratio as well as higher outward migration rate for free water during CUHPD process. The mechanical effect produced by ultrasonic wave could cause the rapid expansion and contraction of moisture inside samples, and the ultrasound's cavitation effect could expand the internal tissue gap and micro-capillaries of materials (Magalhães et al. 2017), thus reducing the resistance of water diffusion and promoting water migration and then speeding up the removal of free water.

With the removal of free water in kiwifruit, immobilized water began to migrate subsequently. It can be seen from Fig. 7 that the immobilized water contents inside kiwifruit increased firstly and then decreased during dehydration process at the four ultrasonic power levels. In the early stage of dehydration, the peak area of immobilized water improved with the extension of drying time. This might be due to the elevation of carbohydrate concentration in kiwifruit caused by the removal of free water in the early period of drying (Cheng et al. 2014), resulting in the difference of cell liquid concentration and the transition of free water to immobilized water under the concentration gradient. When the ultrasonic power was 0, 18, 36, and 54 W, the maximum peak areas of immobilized water appeared at 120, 120, 90, and 60 min, respectively, which elucidated that the increasing in ultrasonic power can not only promote the migration of free water, but also accelerate the transformation from free water to immobilized water. The peak area of immobilized water demonstrated a downward trend in the late drying period, indicating that immobilized water in kiwifruit began to decrease while the free water decreased. This is due to the fact that the free water contained in kiwifruit is not enough, which leads to the gradual slowdown or even stop of the transition to immobilized water. On the other hand, it may also be due to that the continuous effect of ultrasound on the internal organization of the material could reduce the binding force of immobilized water and improve its mobility, causing the continuous outward migration and removal of immobilized water (Zhao et al. 2019). Unlike the complete removal of free water, there was still a small amount of immobilized water (about 7.1–8.4% of the original immobilized water) left inside kiwifruit at the end of drying, which may remain in the cell gap or micro-capillary of kiwifruit with strong binding force and high migration resistance. The peak area proportion of immobilized water improved first and then reduced, and such a phenomenon could be attributed to the removal of free water and the transformation to immobilized water at the first stage of drying and then the migration of immobilized water thereafter.

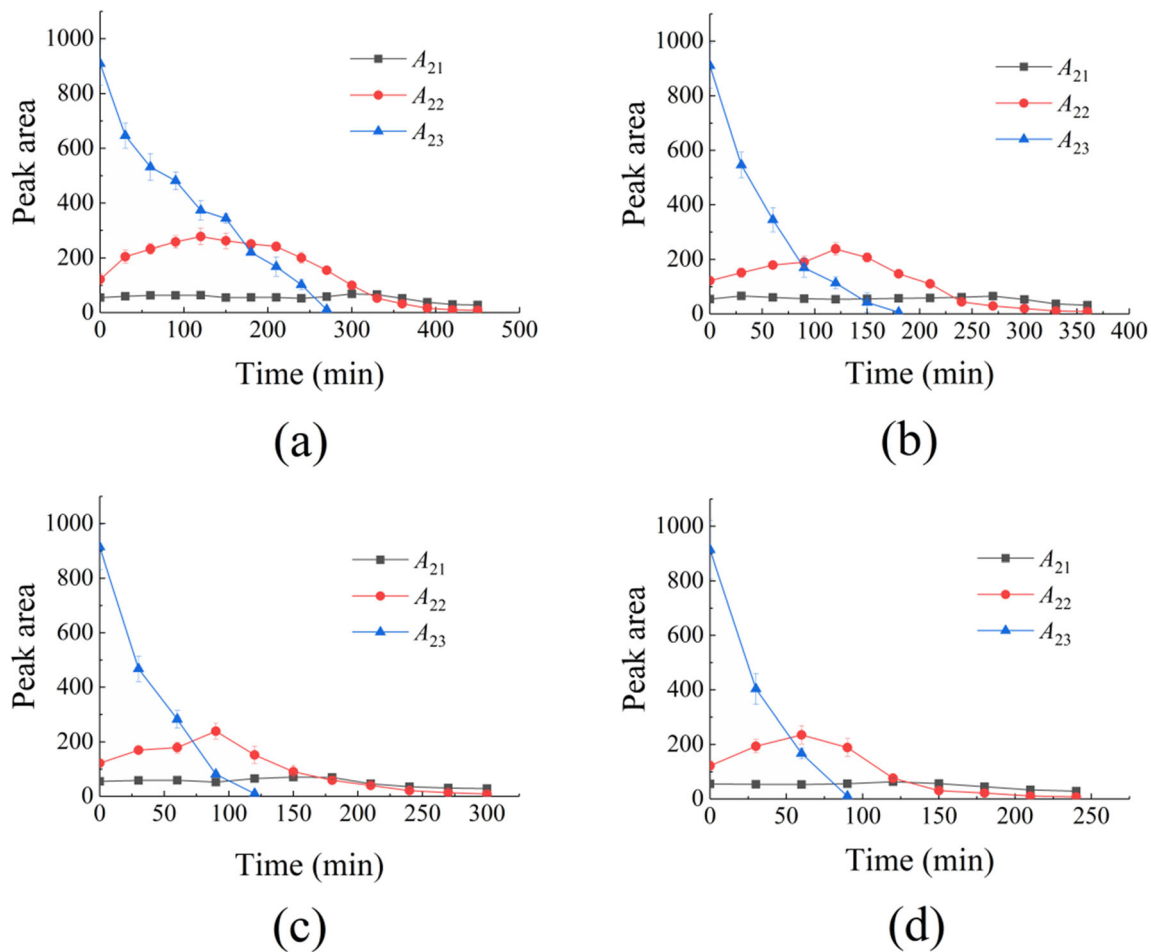


Fig. 7 Changes of peak area of kiwifruit during CUHPD at different ultrasonic powers: **a** 0 W, **b** 18 W, **c** 36 W, **d** 54 W

The peak area and the corresponding proportion of bound water in CUHPD of kiwifruit are demonstrated in Fig. 7 and Fig. 8. Although the content of bound water was very less in fresh kiwifruit, the peak area of bound water increased slowly and then decreased slowly, and the peak proportion increased steadily as drying process went on. In the early period of CUHPD, the amount of bound water (A_{21}) increased with the progress of drying. The decrease of free water content would result in the decrease of cell activity and the increase of tissue fluid concentration in kiwifruit, and promote the formation of bound water by hydrogen bonding with macromolecules (Sun et al. 2017a). In addition, with the removal of free water and the reduction of internal fluidity in kiwifruit, some immobilized water migrated to the cell wall, resulting in the conversion of hydrophilic groups within the cell wall pectin molecule to protons in immobilized water, thus resulting in physical binding water with weak hydrogen bond energy (Xu et al. 2017). At the later period of CUHPD, with the total removal of free water and the continuous decrease of immobilized water, the peak area of bound water began to decline slowly, indicating the reduction of bound water in kiwifruit. This process corresponds to the latter part of drying curves in Fig. 3 with the characteristics of

slow water removal and low drying rate. When the free water was removed totally, the immobilized water and bound water began to be removed, and some bound water with weak bond energy and those bound water produced from the immobilized water bound to pectin macromolecule were gradually removed during drying. At the same time, the thermal decomposition of enzymes and nutrients in the materials can transform part of bound water to immobilized water (Lv et al. 2018). After drying, the bound water left in kiwifruit was 51–59% of that in fresh kiwifruit, and the variation regulations of bound water are similar at the four ultrasonic power levels, which indicates that the improvement of ultrasonic power is not enough to remove most bound water in kiwifruit. It is also seen in Fig. 8 that most of the water left in kiwifruit is bound water, mainly because of its high bond energy, strong binding force, and low degree of freedom (Wei et al. 2018).

Proton Density Image

The proton density image changes of kiwifruit in CUHPD at different ultrasonic powers are demonstrated in Fig. 9, which could visualize the moisture distribution change in kiwifruit

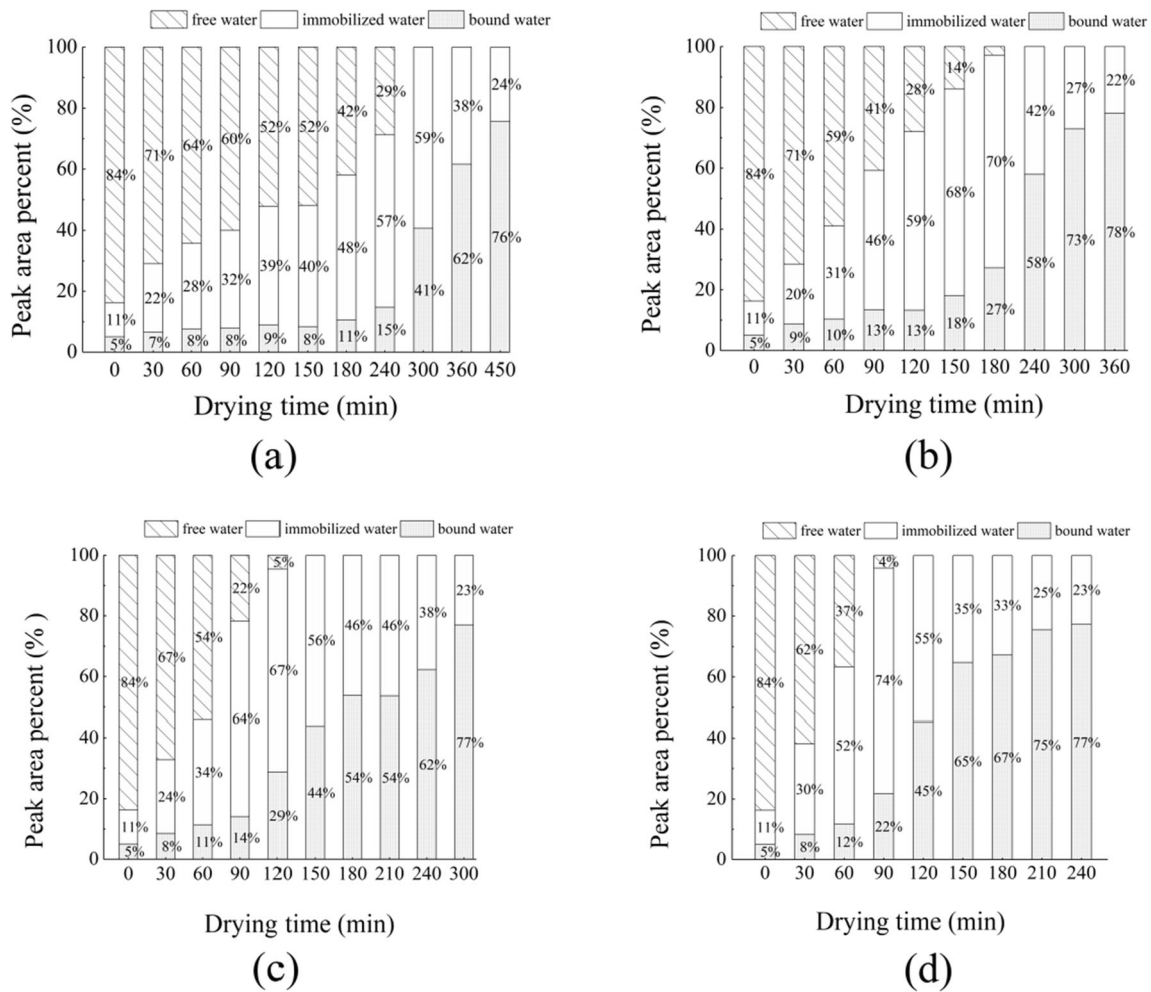


Fig. 8 Changes of peak area proportions of kiwifruit during CUHPD at different ultrasonic powers: a 0 W, b 18 W, c 36 W, d 54 W

during CUHPD process. In the images, higher proton density of gray image and stronger signal represented higher water content in kiwifruit slices, and lower proton density meant less

water content (Xu et al. 2017). It can be observed from Fig. 9 that fresh kiwifruits have high moisture content. With the drying process, the moisture in kiwifruit slices was continuously

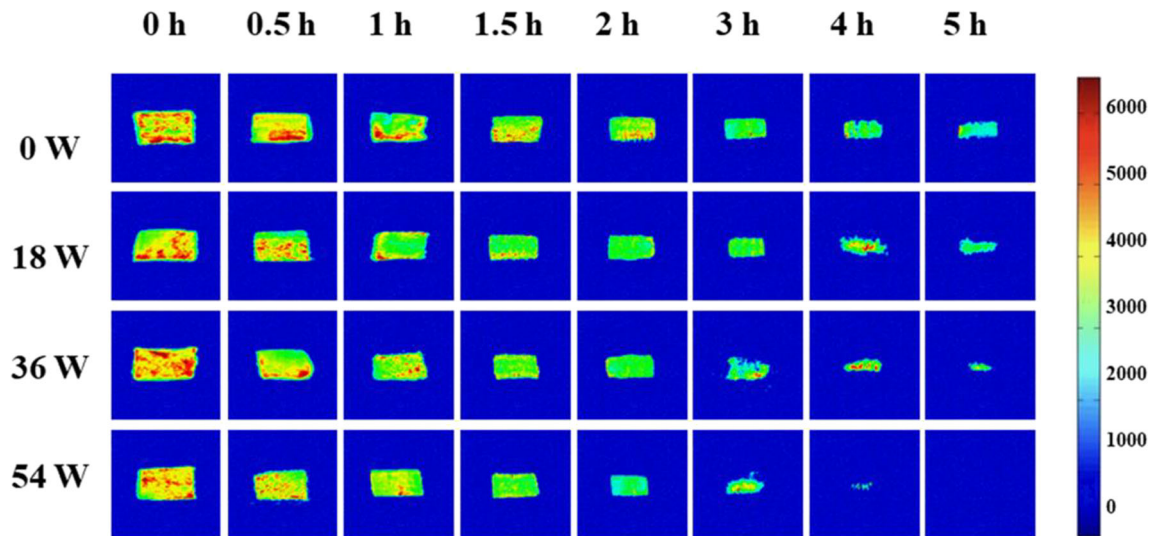


Fig. 9 Proton density image changes of kiwifruit in CUHPD at different ultrasonic powers

removed, and proton density gradually weakened and disappeared from the outside to the inside, indicating that water gradually gathered to the inner layer, and water gradually lost from the outside to the inside. In the latter drying period, the proton density image change inside the materials was relatively slow, representing that internal moisture was more difficult to remove than that in kiwifruit's surface due to high diffusion resistance. At the end of drying, the image was very close to the background color, indicating that the moisture content in kiwifruit was low. Comparing the changes of proton density maps under four different ultrasonic powers conditions, it is found that proton density decreased slowly at 0 W. With the rising in ultrasonic power, the relative proton intensity decreased faster, especially when ultrasonic power was 54 W. The phenomenon indicates that CU application in HPD could remarkably affect the water migration and loss in kiwifruit slices, and higher ultrasonic power could produce stronger intensifying effects and subsequently accelerate moisture migration rate.

Conclusions

The CUHPD experiments of kiwifruit slices were conducted. CU application in HPD of kiwifruit was beneficial to accelerating dehydration rate and shortening drying time. The rise in ultrasonic power could promote internal moisture migration and improve drying rate. Weibull distribution function could simulate CUHPD of kiwifruit with high precision. The obtained α and β values revealed that the improvement of ultrasonic power can improve water removal and transform the moisture diffusion mechanism from total internal moisture diffusion control to partial internal moisture diffusion control. The D_{cal} values increased with the improvement of ultrasonic power, indicating that higher CU power could accelerate water diffusion in kiwifruit. Higher ultrasonic power could produce more micropores and larger microtunnels in the surface microstructure and internal microstructure of kiwifruit.

LF-NMR analysis indicated that free water, immobilized water, and bound water exists in kiwifruit, and the three kinds of water states could migrate and change during CUHPD. Free water with the highest mobility was the most abundant water in kiwifruit, and has the highest removal rate and disappeared first. The contents of immobilized water and bound water gradually increased and then decreased during CUHPD process; however, they could not be completely removed at the end of drying. The rising in ultrasonic power can promote internal water migration and then be conducive to shortening the required dehydration time. Proton density images revealed that CU application at higher ultrasonic power could significantly promote the water diffusion from internal kiwifruit outward the surface during CUHPD, and thereby accelerate water removal as well as dehydration rate.

Funding information The authors are thankful to the financial supporting from the College's Innovation Talents Program in Henan (19HASTIT013) and the Natural Science Program in Henan (162300410100).

References

- Akar, G., & Barutçu Mazı, I. (2019). Color change, ascorbic acid degradation kinetics, and rehydration behavior of kiwifruit as affected by different drying methods. *Journal of Food Process Engineering*, 42(3), e13011. <https://doi.org/10.1111/jfpe.13011>.
- AOAC. (1990). *Official methods of analysis*. Washington, DC: Association of Official Analytical Chemists.
- Çalışkan, G., Ergün, K., & Dirim, S. N. (2015). Freeze drying of kiwi (*Actinidia deliciosa*) puree and the powder properties. *Italian Journal of Food Science*, 27(3), 385–396.
- Chapchaimoh, K., Poomsa-ad, N., Wiset, L., & Morris, J. (2016). Thermal characteristics of heat pump dryer for ginger drying. *Applied Thermal Engineering*, 95, 491–498.
- Cheng, X. F., Zhang, M., Adhikari, B., & Islam, M. N. (2014). Effect of power ultrasound and pulsed vacuum treatments on the dehydration kinetics, distribution, and status of water in osmotically dehydrated strawberry: a combined NMR and DSC study. *Food and Bioprocess Technology*, 7(10), 2782–2792.
- Corzo, O., Bracho, N., & Alvarez, C. (2010). Weibull model for thin-layer drying of mango slices at different maturity stages. *Journal of Food Processing & Preservation*, 34(6), 993–1008.
- Darıcı, S., & Şen, S. (2015). Experimental investigation of convective drying kinetics of kiwi under different conditions. *Heat and Mass Transfer*, 51(8), 1167–1176.
- Fernandes, F. A. N., Rodrigues, S., Cárcel, J. A., & García-Pérez, J. V. (2015). Ultrasound-assisted air-drying of apple (*Malus domestica* L.) and its effects on the vitamin of the dried product. *Food and Bioprocess Technology*, 8(7), 1503–1511.
- García-Pérez, J. V., Cárcel, J. A., Riera, E., Mulet, A., Wu, Z. H., & Mujumdar, A. S. (2009). Influence of the applied acoustic energy on the drying of carrots and lemon peel. *Drying Technology*, 27(2), 281–287.
- García-Pérez, J. V., Ortuño, C., Puig, A., Cárcel, J. A., & Perez-Munuera, I. (2012). Enhancement of water transport and microstructural changes induced by high-intensity ultrasound application on orange peel drying. *Food and Bioprocess Technology*, 5(6), 2256–2265.
- Hii, C. L., Law, C. L., & Suzannah, S. (2012). Drying kinetics of the individual layer of cocoa beans during heat pump drying. *Journal of Food Engineering*, 108(2), 276–282.
- Izli, N., Izli, G., & Taskin, O. (2017). Drying kinetics, colour, total phenolic content and antioxidant capacity properties of kiwi dried by different methods. *Journal of Food Measurement and Characterization*, 11(1), 64–74.
- Jiang, N., Liu, C., Li, D., Zhang, J., Zhang, Z., Huang, J., & Yu, Z. (2018). Effect of thermosonic pretreatment and microwave vacuum drying on the water state and glass transition temperature in *Agaricus bisporus* slices. *Food and Bioprocess Technology*, 11(1), 172–184.
- Kek, S. P., Chin, N. L., & Yusof, Y. A. (2013). Direct and indirect power ultrasound assisted pre-osmotic treatments in convective drying of guava slices. *Food and Bioprocess Technology*, 91(4), 495–506.
- Li, M., Wang, H., Zhao, G., Qiao, M., Mei, L., Sun, L., Gao, X., & Zhang, J. (2014). Determining the drying degree and quality of chicken jerky by LF-NMR. *Journal of Food Engineering*, 139(139), 43–49.
- Li, X., Zhong, Y., Yuan, Y., Liu, Y., & Zhang, Z. (2018). Trypsin and ascorbic acid have a synergistic effect on the quality of apple processing by protecting apple cells from oxidative damage. *Journal of Food Biochemistry*, 42(5), e12582.

- Liu, Y., Wu, J., Miao, S., Chong, C., & Sun, Y. (2014). Effect of a modified atmosphere on drying and quality characteristics of carrots. *Food and Bioprocess Technology*, 7(9), 2549–2559.
- Liu, Y., Sun, Y., Wang, L., Miao, S., Luo, D., Luo, L., & Zhu, W. (2015). Drying characteristics of pear slices during ultrasound-assisted hot air drying. *Food Science*, 36(9), 1–6.
- Liu, Y., Sun, Y., Yu, H., Yin, Y., Li, X., & Duan, X. (2017). Hot air drying of purple-fleshed sweet potato with contact ultrasound assistance. *Drying Technology*, 35(5), 564–576.
- Liu, Y., Zeng, Y., Wang, Q., Sun, C., & Xi, H. (2019). Drying characteristics, microstructure, glass transition temperature, and quality of ultrasound-strengthened hot air drying on pear slices. *Journal of Food Processing and Preservation*, 43(3), e13899.
- Lv, W., Zhang, M., Bhandari, B., Li, L., & Wang, Y. (2017). Smart NMR method of measurement of moisture content of vegetables during microwave vacuum drying. *Food and Bioprocess Technology*, 10(12), 2251–2260.
- Lv, W., Zhang, M., Wang, Y., & Adhikari, B. (2018). Online measurement of moisture content, moisture distribution, and state of water in corn kernels during microwave vacuum drying using novel smart NMR/MRI detection system. *Drying Technology*, 36(13), 1592–1602.
- Magalhães, M. L., Cartaxo, S. J. M., Gallão, M. I., García-Pérez, J. V., Cárcel, J. A., Rodrigues, S., & Fernandes, F. A. N. (2017). Drying intensification combining ultrasound pre-treatment and ultrasound-assisted air drying. *Journal of Food Engineering*, 215, 72–77.
- Marabi, A., Livings, S., Jacobson, M., & Saguy, I. S. (2003). Normalized Weibull distribution for modeling rehydration of food particulates. *European Food Research and Technology*, 217(4), 311–318.
- Mohammadi, I., Tabatabaekolour, R., & Motevali, A. (2019). Effect of air recirculation and heat pump on mass transfer and energy parameters in drying of kiwifruit slices. *Energy*, 17, 149–158.
- Musielak, G., Mierzwa, D., & Kroehnke, J. (2016). Food drying enhancement by ultrasound - a review. *Trends in Food Science & Technology*, 56, 126–141.
- Nowacka, M., Tappi, S., Tylewicz, U., Luo, W., Rocculi, P., Wesoly, M., et al. (2018). Metabolic and sensory evaluation of ultrasound-assisted osmo-dehydrated kiwifruit. *Innovative Food Science & Emerging Technologies*, 50, 26–33.
- Ortuño, C., Pérez-Munuera, I., Puig, A., Riera, E., & Garcia-Perez, J. V. (2010). Influence of power ultrasound application on mass transport and microstructure of orange peel during hot air drying. *Physics Procedia*, 3(1), 153–159.
- Rodríguez, Ó., Llabrés, P. J., Simal, S., Femenia, A., & Rosselló, C. (2015). Intensification of predrying treatments by means of ultrasonic assistance: effects on water mobility, PPO activity, microstructure, and drying kinetics of apple. *Food and Bioprocess Technology*, 8(3), 503–515.
- Rojas, M. L., & Augusto, P. E. D. (2018). Ethanol and ultrasound pre-treatments to improve infrared drying of potato slices. *Innovative Food Science and Emerging Technologies*, 49, 65–75.
- Schössler, K., Jäger, H., & Knorr, D. (2012). Novel contact ultrasound system for the accelerated freeze-drying of vegetables. *Innovative Food Science & Emerging Technologies*, 16, 113–120.
- Sun, Y., Liu, Y., Yu, H., Xie, A., Li, X., Yin, Y., & Duan, X. (2017a). Non-destructive prediction of moisture content and freezable water content of purple-fleshed sweet potato slices during drying process using hyperspectral imaging technique. *Food Analytical Methods*, 10(5), 1535–1546.
- Sun, X. F., Zhu, W. X., Li, X. L., & Fan, J. L. (2017b). Effects of heat pump drying temperature and dietary fat on carrot β -carotene bio-accessibility. *International Journal of Agricultural & Biological Engineering*, 10(4), 234–242.
- Sun, Q., Zhang, M., Mujumdar, A. S., & Yang, P. (2019). Combined LF-NMR and artificial intelligence for continuous real-time monitoring of carrot in microwave vacuum drying. *Food and Bioprocess Technology*, 12(4), 551–562.
- Tao, Y., Han, M., Gao, X., Han, Y., Show, P. L., Liu, C., Ye, X., & Xie, G. (2019). Applications of water blanching, surface contacting ultrasound-assisted air drying, and their combination for dehydration of white cabbage: drying mechanism, bioactive profile, color and rehydration property. *Ultrasonics Sonochemistry*, 53, 192–201.
- Uribe, E., Vega-Gálvez, A., Oyanadel, R., Torrico, J. S., & Miranda, M. (2011). Characteristics of convective drying of Pepino fruit (*Solanum muricatum* Ait.): application of Weibull distribution. *Food and Bioprocess Technology*, 4(8), 1349–1356.
- Vallespir, F., Cárcel, J. A., Marra, F., Eim, V. S., & Simal, S. (2018). Improvement of mass transfer by freezing pre-treatment and ultrasound application on the convective drying of beetroot (*Beta vulgaris* L.). *Food and Bioprocess Technology*, 11(1), 72–83.
- Vallespir, F., Crescenzo, L., Rodríguez, Ó., Marra, F., & Simal, S. (2019). Intensification of low-temperature drying of mushroom by means of power ultrasound: effects on drying kinetics and quality parameters. *Food and Bioprocess Technology*, 12(5), 839–851.
- Wei, S., Tian, B. Q., Jia, H. F., Zhang, H. Y., He, F., & Song, Z. P. (2018). Investigation on water distribution and state in tobacco leaves with stalks during curing by LF-NMR and MRI. *Drying Technology*, 36(12), 1515–1522.
- Weibull, W. (1951). A statistical distribution of wide applicability. *Journal of Applied Mechanics*, 18(2), 293–297.
- Winiczenko, R., Górnicki, K., Kaleta, A., Janaszek-Mańkowska, M., & Trajer, J. (2018). Multi-objective optimization of the apple drying and rehydration processes parameters. *Emirates Journal of Food and Agriculture*, 30(1), 1–9.
- Xu, F., Jin, X., Zhang, L., & Chen, X. D. (2017). Investigation on water status and distribution in broccoli and the effects of drying on water status using NMR and MRI methods. *Food Research International*, 96, 191–197.
- Zhao, H., Zhao, Y., & Tao, Z. (2017). Drying kinetics of continuous and intermittent heat pump drying of green soybean seeds. *International Journal of Food Engineering*, 13(11), 20170182.
- Zhao, Y., Bi, J., Zhao, Y., Yi, J., Njoroge, D. M., Peng, J., & Hou, C. (2019). Comparison of dynamic water distribution and microstructure formation of shiitake mushrooms during hot air and far infrared radiation drying by low-field nuclear magnetic resonance and scanning electron microscopy. *Journal of the Science of Food and Agriculture*, 99(6), 2826–2834.